THE JOURNAL OF BIOLOGICAL CHEMISTRY VOL. 284, NO. 32, pp. 21265–21269, August 7, 2009

Helix Straightening as an Activation Mechanism in the Gelsolin Superfamily of Actin Regulatory Proteins*[S]

Received for publication, March 20, 2009, and in revised form, May 11, 2009 Published, JBC Papers in Press, June 1, 2009, DOI 10.1074/jbc.M109.019760

Hui Wang[‡], Sakesit Chumnarnsilpa[§¶], Anantasak Loonchanta[‡], Qiang Li[‖], Yang-Mei Kuan[§], Sylvie Robine[**], Mårten Larsson[§], Ivana Mihalek[‖], Leslie D. Burtnick[‡1], and Robert C. Robinson[§]

*From the [‡]Department of Chemistry and Centre for Blood Research, Life Sciences Institute, University of British Columbia, Vancouver, British Columbia V6T 1Z1, Canada, the [§]Institute of Molecular and Cell Biology, A*STAR, 61 Biopolis Drive, Proteos, Singapore 138673, the [¶]Institutionen för Medicinsk Biokemi och Mikrobiologi, Uppsala University, Box 582, 751 23 Uppsala, Sweden, the [‖]Bioinformatics Institute, A*STAR, 30 Biopolis Drive, Matrix, Singapore 138671, and **UMR 144, Institut Curie, 26 rue d'Ulm, 75248 Paris Cedex 05, France*

Villin and gelsolin consist of six homologous domains of the gelsolin/cofilin fold (V1–V6 and G1–G6, respectively). Villin differs from gelsolin in possessing at its C terminus an unrelated seventh domain, the villin headpiece. Here, we present the crystal structure of villin domain V6 in an environment in which intact villin would be inactive, in the absence of bound Ca^{2+} or phosphorylation. The structure of V6 more closely resembles that of the activated form of G6, which contains one bound Ca^{2+}, rather than that of the calcium ion-free form of G6 within intact inactive gelsolin. Strikingly apparent is that the long helix in V6 is straight, as found in the activated form of G6, as opposed to the kinked version in inactive gelsolin. Molecular dynamics calculations suggest that the preferable conformation for this helix in the isolated G6 domain is also straight in the absence of Ca^{2+} and other gelsolin domains. However, the G6 helix bends in intact calcium ion-free gelsolin to allow interaction with G2 and G4. We suggest that a similar situation exists in villin. Within the intact protein, a bent V6 helix, when triggered by Ca^{2+}, straightens and helps push apart adjacent domains to expose actin-binding sites within the protein. The sixth domain in this superfamily of proteins serves as a keystone that locks together a compact ensemble of domains in an inactive state. Perturbing the keystone initiates reorganization of the structure to reveal previously buried actin-binding sites.

Actin is crucial to such processes as cell movement, cell division, and apoptosis, which are regulated by numerous actin-binding proteins, including gelsolin, Arp2/3, and profilin (for review, see Ref. 1). Gelsolin, the most potent actin filament-severing protein known, can bind to, sever, cap, and nucleate actin filaments in a calcium-, pH-, ATP-, and phospholipid-dependent manner (for review, see Ref. 2). Villin, found in microvilli of absorptive epithelium, is a second member of the gelsolin family of actin-binding proteins. In addition to standard gelsolin-type activities, villin is able to bundle actin filaments and is subject to regulation by tyrosine phosphorylation as well as by Ca^{2+} and phosphatidylinositol 4,5-bisphosphate (for review, see Ref. 3). Many comparisons have been made between gelsolin and villin. The two share 50% amino acid sequence identity and show similar proteolytic cleavage patterns (4). Both contain six similarly folded domains, but villin possesses a seventh domain at its C terminus, the headpiece (HP)[2] domain, which folds into a compact structure that introduces a second F-actin-binding site into the protein. Recent studies indicate that villin uses the HP F-actin-binding sites to achieve bundling (5). In an environment devoid of free Ca^{2+}, gelsolin and villin assume inactive conformations. After binding Ca^{2+}, both undergo conformational rearrangements that expose their binding sites for F-actin. In villin, this includes revealing the HP actin-binding site through a "hinge mechanism" (6).

Biochemical and structural studies have revealed eight Ca^{2+}-binding sites of two types in gelsolin (for review, see Ref. 7). Each of the six domains contains a complete and evolutionarily conserved site, termed type 2, whereas G1 and G4 provide partial Ca^{2+} coordination at interfaces with actin through sites termed type 1. Sequential mutagenesis of these sites in villin has identified six functional Ca^{2+}-binding sites (8): two major sites, one each of type 1 and type 2, in V1, plus four type 2 sites in V2–V6. The type 1 site in V1 regulates F-actin-capping and F-actin-severing activities, whereas the lower affinity type 2 site in V1 only affects severing (9). The other four sites are involved in stabilizing villin conformation, but they do not directly influence actin-severing activity. NMR studies of a fragment of villin that consists of V6 and the HP domain have implicated V6 residues Asn^{647}, Asp^{648}, and Glu^{670} in binding Ca^{2+} (10). These

* This work was supported in part by a grant-in-aid from the Heart and Stroke Foundation of British Columbia and Yukon (to L. D. B.) and the Biomedical Research Council of A*STAR (to R. C. R. and I. M.). Funding for the University of British Columbia Centre for Blood Research X-ray Crystallography Hub is provided in part by grants from the Canada Foundation for Innovation, the Michael Smith Foundation for Health Research, the Howard Hughes Medical Institute, and the Canadian Institutes of Health Research. Portions of this research were carried out at the National Synchrotron Radiation Research Center, Taiwan, China, supported by the National Science Council of Taiwan. The Synchrotron Radiation Protein Crystallography Facility is supported by the Taiwan National Research Program for Genomic Medicine.

[S] The on-line version of this article (available at http://www.jbc.org) contains supplemental Figs. 1 and 2, Table 1, and "Experimental Methods."

The atomic coordinates and structure factors (code 3fg7) have been deposited in the Protein Data Bank, Research Collaboratory for Structural Bioinformatics, Rutgers University, New Brunswick, NJ (http://www.rcsb.org/).

[1] To whom correspondence should be addressed: Dept. of Chemistry, 2036 Main Mall, University of British Columbia, Vancouver, BC V6T 1Z1, Canada. Tel.: 604-822-4767; Fax: 604-822-2847; E-mail: burtnick@chem.ubc.ca.

[2] The abbreviations used are: HP, headpiece; G1–G6, gelsolin domains 1–6; V1–V6, villin domains 1–6.

experiments also revealed the first 80 residues of V6 to undergo significant conformational change as a result of Ca^{2+} binding.

Nanomolar to micromolar concentrations of free Ca^{2+} govern the actin-binding activities of gelsolin. In contrast, micromolar and millimolar concentrations of calcium ions are required for villin to exhibit capping and severing, respectively. However, after tyrosine phosphorylation, villin can sever actin filaments even at nanomolar Ca^{2+} concentrations (11). Furthermore, although the actin-severing ability of the N-terminal half of villin is calcium-dependent, that by the N-terminal half of gelsolin is not. In contrast, the binding of G-actin of the C-terminal half of both villin and gelsolin requires Ca^{2+}. Creation of hybrid proteins demonstrated that the domains of villin and gelsolin are not interchangeable (12).

Abundant x-ray crystallographic structural information exists for gelsolin, including the calcium ion-free (Ca^{2+}-free), inactive structure of the intact protein (13), the activated N- and C-terminal halves, each in a bimolecular complex with actin (7, 14), and the activated C-terminal half on its own (15, 16). Structural data for intact villin are unavailable and are limited to fragment V1 (17), solved using NMR methods, and the HP domain, solved by NMR and x-ray crystallography (18, 19). NMR experiments also indicate that HP is connected to V6 by a 40-residue disordered linker. As a result, HP has been proposed to bind actin independently of the remainder of the protein (10).

In this report, we present the structure of Ca^{2+}-free, isolated villin V6, which exhibits a typical gelsolin domain fold. The long helix in V6 in this structure is straight, unlike the corresponding helix in G6 of intact Ca^{2+}-free gelsolin, which is bent, and only straightens on calcium activation of the intact protein. Hence, V6 appears to be in an active conformation in the absence of Ca^{2+}. Molecular dynamics simulations indicate that the preferred state of the long helix is also straight for isolated G6 in the absence of Ca^{2+}. Furthermore, they suggest a bistable mechanism of helix conformational change regulated by the presence of the remaining domains, by calcium ions, and by other interactants. We therefore propose a mechanism for the gelsolin family proteins whereby Ca^{2+} triggers the straightening of the domain 6 helix in the native conformation of the inactive proteins to propagate more widespread conformational changes.

EXPERIMENTAL PROCEDURES

Protein Production—Villin domains V4–V6 with an N-terminal 8-histidine tag was expressed in *Escherichia coli* from the expression vector pSY5 and purified through sequential Ni^{2+} affinity and gel filtration chromatographies (see supplemental "Experimental Methods"). Actin was purified from rabbit skeletal muscle by a modified method of Spudich and Watt (20). Villin V4–V6 in 10 mM Tris-HCl, 150 mM NaCl, and 5 mM $CaCl_2$, pH 7.5, was added to actin in 2 mM Tris-HCl, 0.2 mM $CaCl_2$, 0.2 mM ATP, 1 mM dithiothreitol, pH 7.6–7.8 (buffer A), to a molar ratio of 1:1. The resulting solution was held at 4 °C overnight prior to gel filtration (Bio-Rad Sephacryl S300, 90 × 2.5 cm) with elution by buffer A. The fractions containing the protein complex were pooled and concentrated to 10 mg/ml, as determined by UV absorbance at 280 nm (PerkinElmer Life Sciences Lamda 4B) using a calculated absorption coefficient of 1.4 ml mg^{-1} cm^{-1}.

Crystallization and Data Collection—Crystals were grown at 4 °C using the hanging-drop vapor diffusion method. The protein solution (10 mg/ml) was mixed in a 1:1 ratio (v/v) with a reservoir solution containing 15% (w/v) polyethylene glycol 8000, 100 mM sodium acetate buffer, pH 5.0. Crystals required 3–4 weeks of incubation to grow to a suitable quality for diffraction analysis. Prior to x-ray data collection, the crystals were transferred into a cryoprotectant solution, 25% (v/v) glycerol, 15% (w/v) polyethylene glycol 8000, 100 mM sodium acetate buffer, pH 5.0, and flash-frozen in liquid nitrogen.

Diffraction data initially were collected to a resolution of 3.0 Å using a Rigaku MM007HF rotating copper anode source with OSMIC VariMaxHR mirrors and a MAR345 image plate detector at the University of British Columbia Centre for Blood Research (Vancouver, Canada). Data were indexed, integrated, and scaled using HKL2000 software (21). Subsequently, data were collected to a resolution of 2.0 Å using an Area Detector Systems Corp. Quantum-315 charge-coupled device detector on beamline BL31B1 at the National Synchrotron Radiation Research Center (Taiwan, China; supplemental Table 1).

Structure Solution and Refinement—Structural analysis was initiated by molecular replacement using single domains G4–G6 (from Protein Data Bank code 1p8x) as a model. An unambiguous solution showed that the diffraction originated solely from V6, with the V4 and V5 domains and actin not evident. The crystallographic asymmetric unit contains two V6 domains, which permits calculation of a solvent content of 55%. Refinement was carried out using the CCP4 suite of crystallographic programs (22).

Molecular Dynamics Simulations—To monitor the relaxation of G6 isolated from the context of intact Ca^{2+}-free gelsolin, five simulations were initiated from residues 640–731 (G6) excised from the inactive structure of gelsolin (Protein Data Bank code 1d0n) (13). Two control runs, meant to assure that the long helix does not bend spontaneously in the isolated domain, were initiated from residues 640–742 (G6) excised from the activated form of the C-terminal half of gelsolin (Protein Data Bank code 1h1v) (14). All simulations were performed using GROMACS version 3.3.3. The force field used was OPLS-AA, with time steps of 2 fs, at a temperature of 300 K, with Berendsen pressure coupling and a pressure of 1 bar. Water was simulated explicitly using the simple point charge model, and Na^+ cations were added as counterions, as needed to render the system electrostatically neutral. The water box size was set to 0.9 nm from the protein surface. Energy minimization lasted 6 ps, and frames were sampled every 100 ps.

RESULTS

Structural Comparison of V6 with G6—Fig. 1*A* represents the structure of V6 determined at 2-Å resolution. Like gelsolin G6, V6 consists of a five-stranded β-sheet at its core sandwiched between a pair of α-helices, a long helix that runs roughly parallel and a short helix that lies perpendicular to the strands. There is no calcium ion bound to V6 in this structure. Because the amino acid sequence of V6 is ~50% identical with that of G6, the folding and functions of these two domains invite direct comparison. Of the six domains of gelsolin, the structure of V6

most closely resembles that of G6 in its calcium ion-bound (Ca^{2+}-bound) form (Fig. 1*C*) (root mean square deviation of C-α positions for 99 residues = 0.96 Å). The long helix in V6 and the Ca^{2+}-bound form of G6 is in an extended state, in contrast to the kinked state observed in G6 in the context of its intact Ca^{2+}-free parent protein (Fig. 1*E*). Comparison of the arrangement of the residues important in binding Ca^{2+} in G6 (Ser^{646}, Asn^{647}, Asp^{670}, and Glu^{692}; Fig. 1*D*) with that of the homologous residues from V6 (Ser^{625}, Asn^{626}, Asp^{648}, and Glu^{670}; Fig. 1*B*) emphasizes the structural similarity to Ca^{2+}-bound G6. By contrast, in Ca^{2+}-free G6, the positions and interactions of these residues are altered significantly (Fig. 1*F*). These comparisons suggest that the present structure of V6 isolated from the rest of the villin domains is that of an activated state despite the absence of bound Ca^{2+}.

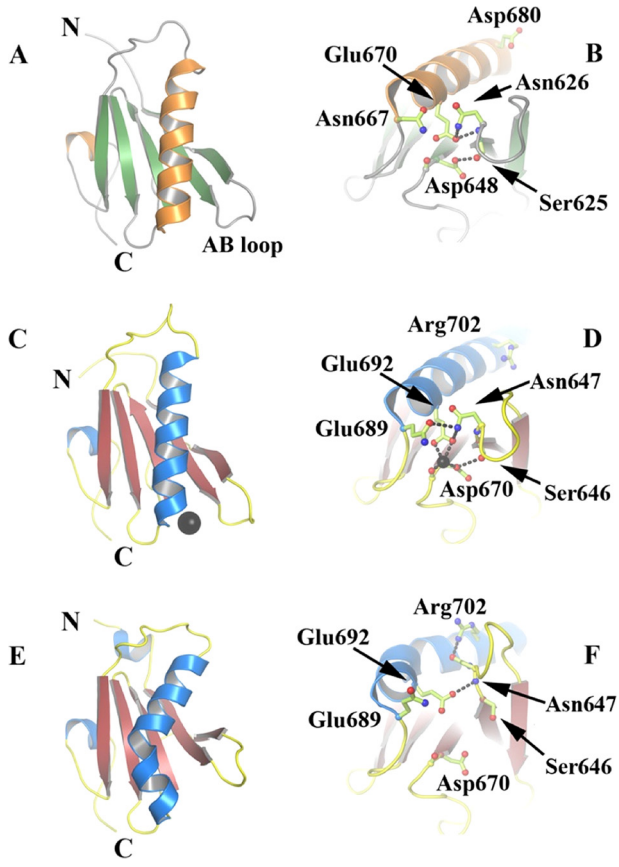

FIGURE 1. **Structural comparison of villin V6 (Ca^{2+}-free) with gelsolin G6 (Ca^{2+}-bound and Ca^{2+}-free).** *A*, schematic representation of isolated Ca^{2+}-free V6. *B*, key residues that are involved in the putative V6 calcium-binding site, viewed from below with respect to *A*. *C* and *D*, Ca^{2+}-bound form of gelsolin G6, displaying a straight helix, taken from the Ca^{2+}-bound form of G4–G6 (Protein Data Bank code 1p8x). *E* and *F*, Ca^{2+}-free form of G6 revealing a kinked helix and a translocated AB loop, taken from the structure of whole plasma gelsolin (Protein Data Bank code 1d0n). The Ca^{2+}-binding residues are dislocated in the absence of Ca^{2+} compared with *D*. A hydrogen bond between Asn^{647} and Arg^{702} links the bending of the helix to movement of the AB loop. Protein representations were generated here and in the figures that follow using PyMOL.

V6 Interaction Interfaces—G6 is the central domain in inactive Ca^{2+}-free gelsolin, forming direct contacts with all other domains (13). G6 interacts most extensively with G2 and G4 (Fig. 2*A*). Of particular note is a continuous β-sheet between G4 and G6 that seals the G4–G6 latch, obscuring the actin-binding site on G4. Although binding Ca^{2+} triggers disruption of this latch, it causes only subtle changes at the G6 interface with G4 (Fig. 2, compare *B* and *C*). There is on the surface of V6 (Fig. 2*D*) a region sufficiently similar to that on Ca^{2+}-free G6, as portrayed in Fig. 2*B*, to suggest that interaction with the edge of the core β-sheet of V4 may occur, as observed between G6 and G4. However, models for the loop that exits the domain 4 strand indicate small steric clashes with both Ca^{2+}-bound G6 (Fig. 2*C*) and Ca^{2+}-free V6 (Fig. 2*D* and supplemental Fig. 1), suggesting that binding of domain 6 to domain 4 would be unfavorable in these two conformations. Surface residues at this interface, including residues involved in the steric clash, show conservation within, yet divergence between, gelsolins and villins (supplemental Fig. 1). Taken together, these data suggest that the manner in which V6 interacts with V4 in villin is analogous with that in which G6 interacts with G4 in gelsolin, yet displays aspects of uniqueness. Most notably, Ca^{2+}-free V6 in isolation adopts an activated conformation.

In inactive gelsolin, electrostatic interactions between a negatively charged surface on G6, which includes Asp^{670}, with Arg^{168} and Arg^{169} (in G2) (Figs. 2*A* and 3*A*), fasten the tail latch over the F-actin-binding site of G2 (14, 23). Coordination of a Ca^{2+} by G6 requires participation of the side chain of Asp^{670}, leading to the disruption of these interactions (Fig. 1, compare *D* and *F*). These residues are conserved in villin (Asp^{648}, Lys^{145}, and Arg^{146}, respectively; Fig. 1*B*). Furthermore, surface residues at the interface with the N-terminal half display conservation within, yet divergence between, gelsolins and villins (supplemental Fig. 2). This suggests that V6 will form similar but specific interactions with V1–V3 compared with those seen between G6 and G1–G3. Superposition of the Ca^{2+}-bound structure of G6 (Fig. 3*B*) and the Ca^{2+}-free form of V6 (Fig. 3*C*) onto the structure of Ca^{2+}-free G6 bound to G2 (Fig. 3*A*, coordinates excised from Protein Data Bank code 1d0n) allows the effects of conformational variation in domain 6 in

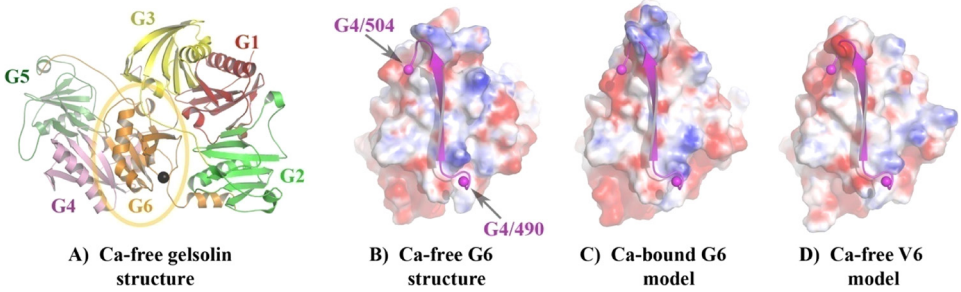

FIGURE 2. **Comparison of the domain 4 interaction surfaces of G6 and V6.** *A*, representation of Ca^{2+}-free gelsolin showing the central position of G6 within the inactive structure. The *black sphere* pinpoints the unoccupied Ca^{2+}-binding site within G6. *B*, surface charge representation of G6 from *A*, rotated ~90° around the vertical axis, showing the interaction surface with G4 via a common β-sheet. *C* and *D*, Ca^{2+}-bound G6 (*C*) and Ca^{2+}-free V6 (*D*) superimposed on G6 in *B*. These models show minor steric clashes with the G4 loop that follows the β-sheet interaction in *B* while the alternating charge distribution at the β-strand edge is maintained.

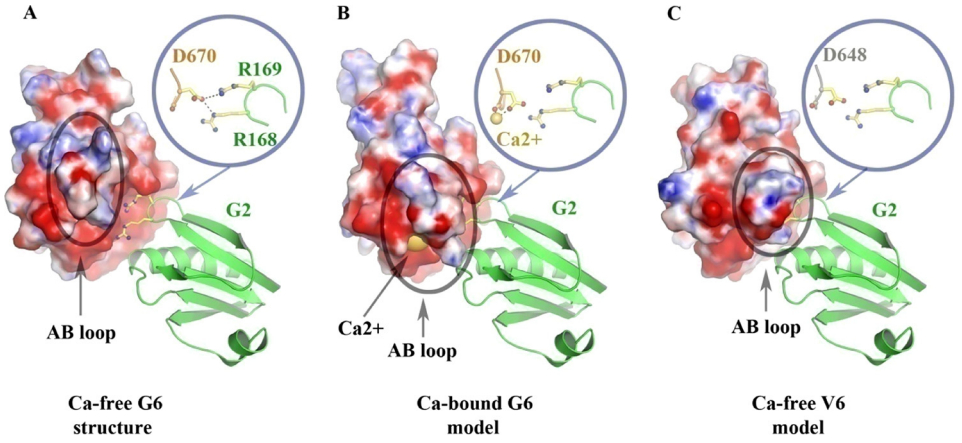

FIGURE 3. **Comparison of the domain 2 interaction surfaces of G6 and V6.** *A*, Arg^{168} and Arg^{169}, from G2, bind to Asp^{670} and a negatively charged surface on G6 in the Ca^{2+}-free form of gelsolin. The AB loop is distant from G2 in this conformation. *B*, Ca^{2+} binding by G6 involves direct coordination with Asp^{670}. Superposition of Ca^{2+}-bound G6 on *A* reveals that the AB loop moves to clash with G2 in this model. *C*, superposition of Ca^{2+}-free V6 on *A* creates a model that demonstrates that Asp^{648} is similarly placed to activate villin via Ca^{2+} binding or to secure the Ca^{2+}-free structure through binding to V2. In this model, the AB loop clashes with domain 2 and, as such, would have to move to bind V2.

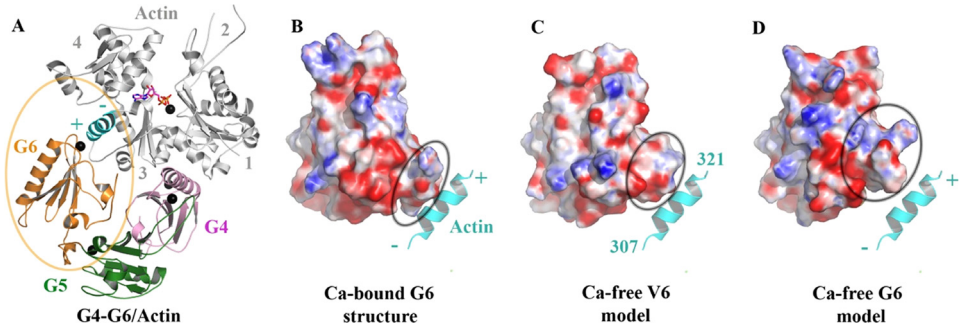

FIGURE 4. **Domain 6 interactions with actin.** *A*, the structure of G4–G6·actin (Protein Data Bank code 1h1v) shows that the actin helix comprising residues 307–321 contacts the AB loop of G6. *B*, surface charge representation of Ca^{2+}-bound G6 shows the interaction with actin residues 307–321. Ca^{2+}-bound G6 is oriented as in Fig. 1*C*. *C*, superposition of Ca^{2+}-free V6 onto *B* produces a model that suggests that V6 might retain the ability to interact with these actin residues. *D*, similar modeling of the transformation of G6 to a Ca^{2+}-free state disturbs that interaction.

gelsolin family members to be assessed with regard to interaction with domain 2. The AB loop within domain 6 adopts different conformations in the presence of the straight *versus* kinked version of its long helix (Fig. 1, compare *A* and *C* with *E*). Movement of the AB loop to go from the Ca^{2+}-free to the Ca^{2+}-bound form of G6 is sterically incompatible with binding of G6 to G2 (Fig. 3, compare *A* and *B*) and likely is a major factor in the separation of G6 and G2 during activation of gelsolin by Ca^{2+}. Similarly, the AB loop in Ca^{2+}-free isolated V6 shows steric clashes in the model presented in Fig. 3*C*, suggesting a similarity in the activation mechanisms for gelsolin and villin. During deactivation, movement of the AB loop may be needed, in combination with bending of the long helix, for V6 to adopt an inactive conformation within whole villin.

In the G4–G6·actin complex (Protein Data Bank code 1h1v), there is interaction between the AB loop of G6 and an α-helical section of peptide chain (residues 307–321) in actin subdomain 3 (Fig. 4, *A* and *B*). This contact arises during the actin filament-severing process and contributes to disruption of actin-actin contacts during that process (14, 23). Superimposition of the coordinates for Ca^{2+}-free G6 from inactive intact gelsolin onto those for Ca^{2+}-bound G6 in the activated structure of the G4–G6·actin complex (Fig. 4*D*) reveals how a transformation of G6 in this complex to a Ca^{2+}-free state would disturb the interaction with actin. However, superimposition of the coordinates of Ca^{2+}-free V6 onto those for Ca^{2+}-bound G6 in G4–G6·actin suggests that contact between V6 and the actin helix could be maintained (Fig. 4*C*). From this, we infer that domain 6 from this family of proteins, once freed of interactions that prevent straightening of its long helix, may bind actin and induce severing at suboptimal calcium concentrations.

Isolating G6 Relieves Constraints on Its Long Helix—Prompted by the apparent anomaly that Ca^{2+}-free V6 should resemble more closely the Ca^{2+}-bound form of G6 rather than the Ca^{2+}-free one, we investigated whether G6 itself would favor such a conformation when isolated from the rest of the gelsolin structure and free of calcium ions. We ran a set of molecular dynamics simulations using the inactive conformation of G6 as the starting point. Four of five trajectories ended in the active-like conformation with the long helix straight in less than 100 ns (Fig. 5, *B* and *C*), whereas the fifth remained bent for the entire 100 ns. In the set of control runs using the active conformation of G6 as the start point, the helix was never observed to return to the bent state (Fig. 5, *A* and *C*), indicating that the conformation with the long helix straight is the preferred state for the isolated domain. Analogously, in the present structure of V6, in the absence of V4 there is no need for the helix to assume the energetically less favored kinked form.

DISCUSSION

The data presented here are consistent with the actin filament-binding, -severing, and -capping mechanisms of gelsolin and villin being very similar. The role of binding Ca^{2+}, in the context of the whole protein, is to release interdomain contacts. One consequence of this is the straightening of otherwise bent α-helices, which we speculate aids in opening latches that would otherwise block actin-binding surfaces.

The kink in the helix of the Ca^{2+}-free G6 can be understood in terms of the context in which it was discovered, folded within the compact globular structure of intact Ca^{2+}-free gelsolin (Fig. 2*A*) (13). The evidence above enforces predictions from sequence alignments that the structures of gelsolin and the V1–V6 body of villin are homologous. As such, the long helix of V6 within Ca^{2+}-free villin may well be bent. During activation, the extended β-sheet shared between G4 and G6 and the inter-

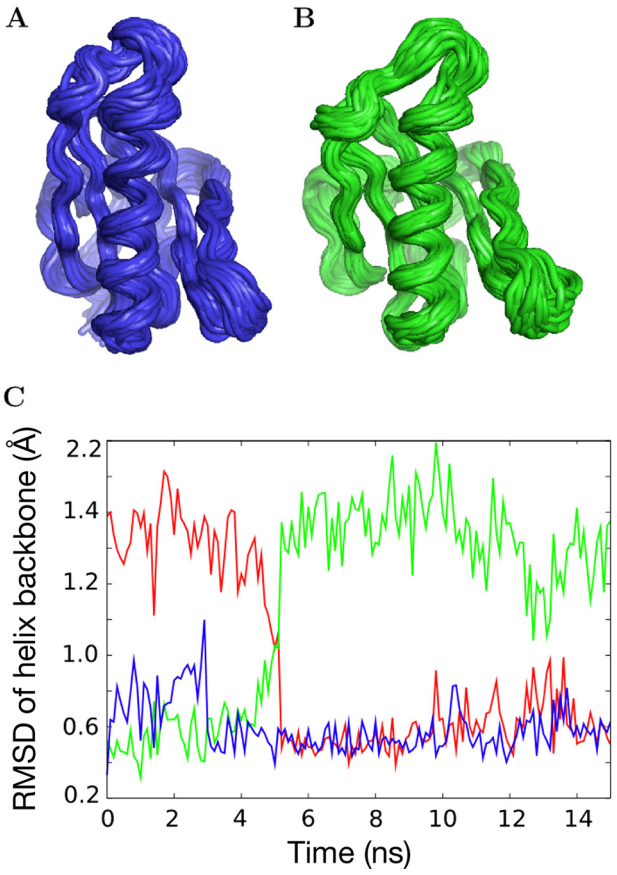

FIGURE 5. **Straightening of the G6 helix in isolation.** *A*, superposition of backbone configurations in 10 ns of a molecular dynamics trajectory in which the initial structure was the active form of G6 (from Protein Data Bank code 1h1v). *B*, superposition of backbone configurations in the last 10 ns (after relaxation to the straightened helix conformation) of a molecular dynamics trajectory, shown in *C*, in which the initial structure was the inactive form of G6 (from Protein Data Bank code 1d0n). *C*, fit of the long helix to the initial, bent conformation (*green*) and to the straightened helix (from Protein Data Bank code 1h1v) (*red*) over a 15-ns molecular dynamics simulation that started with the conformation from Protein Data Bank code 1d0n. As a control, the fit to the straight helix (from Protein Data Bank code 1h1v) is also shown for a simulation starting from the same structure (*blue*). In this trajectory, produced in the absence of other gelsolin domains and Ca^{2+}, the long helix relaxes toward the crystallographic structure of activated G6 (from Protein Data Bank code 1h1v) in less than 10 ns. *RMSD*, root mean square deviation.

action between G2 and G6 (and V4, V2 with V6) are torn apart. The energy cost to do so may be recouped from the binding of calcium ions (Fig. 1*D*), from the formation of new contacts, such as between G5 and G6 (14, 23), and from the straightening of the kinked helix of G6 and, by analogy, V6.

Although helix straightening is shared among gelsolin family members during activation of their abilities to sever and cap actin filaments, differences among the proteins contribute to unique aspects of their functions. For example, activation of the villin HP domain to bundle actin filaments involves a hinged motion away from the gelsolin-like portion of the protein (6). How this is coupled with other stages of activation remains to be explained.

Millimolar calcium ion concentrations, such as those present in blood plasma, activate gelsolin to be extremely efficient at severing undesirable extracellular actin filaments. Such concentrations of free Ca^{2+} are not attainable intracellularly, yet gelsolin is able to regulate actin filaments in this environment. In addition, at low pH, gelsolin is able to sever actin in the complete absence of free Ca^{2+}. Furthermore, villin has calcium requirements for activation quite different from those of gelsolin (8, 9). The importance of Ca^{2+} in activation of members of this protein superfamily appears to vary with both protein identity and environmental setting, despite the high degree of conservation in Ca^{2+}-binding residues.

The structure of Ca^{2+}-free V6 presented in this report and its similarity to that of Ca^{2+}-bound G6 suggest an explanation for the diversity of activating conditions. V6 and G6 may adopt active conformations in the absence of Ca^{2+}, when isolated from the other domains that compose their respective proteins, as a result of a built-in mechanism that involves their long helices. Any process, driven by Ca^{2+} or otherwise, that promotes release of domain 6 from the remaining domains could allow domain 6 to adopt an active conformation and permit the whole protein to interact with actin. We suggest that the long helix in domain 6 and, by analogy the one in domain 3, within this superfamily of proteins can be triggered to straighten under a variety of circumstances.

REFERENCES

1. dos Remedios, C. G., Chhabra, D., Kekic, M., Dedova, I. V., Tsubakihara, M., Berry, D. A., and Nosworthy, N. J. (2003) *Physiol. Rev.* **83,** 433–473
2. McGough, A. M., Staiger, C. J., Min, J. K., and Simonetti, K. D. (2003) *FEBS Lett.* **552,** 75–81
3. Khurana, S., and George, S. P. (2008) *FEBS Lett.* **582,** 2128–2139
4. Janmey, P. A., and Matsudaira, P. T. (1988) *J. Biol. Chem.* **263,** 16738–16743
5. George, S. P., Wang, Y., Mathew, S., Srinivasan, K., and Khurana, S. (2007) *J. Biol. Chem.* **282,** 26528–26541
6. Hesterberg, L. K., and Weber, K. (1983) *J. Biol. Chem.* **258,** 365–369
7. Burtnick, L. D., Urosev, D., Irobi, E., Narayan, K., and Robinson, R. C. (2004) *EMBO J.* **23,** 2713–2722
8. Kumar, N., Tomar, A., Parrill, A. L., and Khurana, S. (2004) *J. Biol. Chem.* **279,** 45036–45046
9. Northrop, J., Weber, A., Mooseker, M. S., Franzini-Armstrong, C., Bishop, M. F., Dubyak, G. R., Tucker, M., and Walsh, T. P. (1986) *J. Biol. Chem.* **261,** 9274–9281
10. Smirnov, S. L., Isern, N. G., Jiang, Z. G., Hoyt, D. W., and McKnight, C. J. (2007) *Biochemistry* **46,** 7488–7496
11. Kumar, N., and Khurana, S. (2004) *J. Biol. Chem.* **279,** 24915–24918
12. Finidori, J., Friederich, E., Kwiatkowski, D. J., and Louvard, D. (1992) *J. Cell Biol.* **116,** 1145–1155
13. Burtnick, L. D., Koepf, E. K., Grimes, J., Jones, E. Y., Stuart, D. I., McLaughlin, P. J., and Robinson, R. C. (1997) *Cell* **90,** 661–670
14. Choe, H., Burtnick, L. D., Mejillano, M., Yin, H. L., Robinson, R. C., and Choe, S. (2002) *J. Mol. Biol.* **324,** 691–702
15. Kolappan, S., Gooch, J. T., Weeds, A. G., and McLaughlin, P. J. (2003) *J. Mol. Biol.* **329,** 85–92
16. Narayan, K., Chumnarnsilpa, S., Choe, H., Irobi, E., Urosev, D., Lindberg, U., Schutt, C. E., Burtnick, L. D., and Robinson, R. C. (2003) *FEBS Lett.* **552,** 82–85
17. Markus, M. A., Matsudaira, P., and Wagner, G. (1997) *Protein Sci.* **6,** 1197–1209
18. Vardar, D., Buckley, D. A., Frank, B. S., and McKnight, C. J. (1999) *J. Mol. Biol.* **294,** 1299–1310
19. Meng, J., Vardar, D., Wang, Y., Guo, H. C., Head, J. F., and McKnight, C. J. (2005) *Biochemistry* **44,** 11963–11973
20. Spudich, J. A., and Watt, S. (1971) *J. Biol. Chem.* **246,** 4866–4871
21. Otwinowski, Z., and Minor, W. (1997) *Methods Enzymol.* **276,** 307–326
22. Collaborative Computational Project 4 (1994) *Acta Crystallogr. D Biol. Crystallogr.* **50,** 760–763
23. Robinson, R. C., Mejillano, M., Le, V. P., Burtnick, L. D., Yin, H. L., and Choe, S. (1999) *Science* **286,** 1939–1942